Accepted Manuscript

The use of inline high-shear rotor-stator mixing for preparation of high-solids milk-protein-stabilised oil-in-water emulsions with different protein:fat ratios

Jonathan J. O'Sullivan, Kamil P. Drapala, Alan L. Kelly, James A. O'Mahony

PII:	S0260-8774(17)30446-6
DOI:	10.1016/j.jfoodeng.2017.10.015
Reference:	JFOE 9048
To appear in:	*Journal of Food Engineering*
Received Date:	09 August 2017
Revised Date:	17 October 2017
Accepted Date:	22 October 2017

Please cite this article as: Jonathan J. O'Sullivan, Kamil P. Drapala, Alan L. Kelly, James A. O' Mahony, The use of inline high-shear rotor-stator mixing for preparation of high-solids milk-protein-stabilised oil-in-water emulsions with different protein:fat ratios, *Journal of Food Engineering* (2017), doi: 10.1016/j.jfoodeng.2017.10.015

Highlights

- Emulsification of different fat-filled milk formulations was investigated.
- Emulsification was achieved using novel inline high-shear mixing technology.
- The emulsification process was monitored inline using pressure drop analysis.
- Pressure drop data allowed for the estimation of viscosity during emulsion formation.

The use of inline high-shear rotor-stator mixing for preparation of high-solids milk-protein-stabilised oil-in-water emulsions with different protein:fat ratios

Jonathan J. O'Sullivan[a,b], Kamil P. Drapala[a,b], Alan L. Kelly[a,b], James A. O'Mahony[a,b]*

[a]School of Food and Nutritional Sciences, University College Cork, Cork, Ireland

[b]Dairy Processing Technology Centre, University College Cork, Cork, Ireland

* Corresponding author: Email address: sa.omahony@ucc.ie

Abstract:

The emulsification of refined palm oil (RPO) in a continuous phase consisting of skim milk concentrate (SMC) and maltodextrin with a dextrose equivalent value of 17 (MD17) to produce fat-filled milk emulsions (FFMEs), was studied. A novel inline high-shear mixing (IHSM) method was used to produce emulsions, and three protein contents were investigated at a fixed RPO content of 12%: low (7.7%), medium (10.5%) and high (13%). Pressure drop measurement was used as an inline approach to determine viscosity using the Hagen-Poiseuille equation. In addition, offline viscometry, particle size and emulsion stability analyses were performed. Emulsion fat droplet size decreased significantly ($P < 0.05$) as a function of number of passes through the IHSM, due to an effective increase in residence time. Furthermore, inline pressure drop data demonstrated that the emulsification process displayed two distinct stages: (i) oil injection, and (ii) reduction in fat droplet size, irrespective of protein content.

Keywords: High solids emulsions, High-shear inline mixer, Pressure drop, Skim milk concentrate, Refined palm oil, Maltodextrin

1. Introduction

Milk is a highly versatile raw material and, over the past century, significant advances have been achieved in its fractionation into a wide variety of components (Fox, 2008; O'Sullivan & O'Mahony, 2016). These constituent-based ingredients are often recombined, sometimes with ingredients derived from other sources (*e.g.*, plant-derived proteins, carbohydrates and lipids), to achieve different formulations, which can be utilised as final products by the consumer (*e.g.*, enriched milk powders), or be further processed as ingredients by food manufacturers (*e.g.*, protein concentrates/isolates or blends, for example in the manufacture of infant formulae) (O'Connell & Flynn, 2007). One such example is fat-filled milk powders (FFMPs), which are dried protein-stabilised emulsions, typically produced by solids concentration (*e.g.*, by evaporation) and homogenisation followed by spray drying. These systems are intended either for direct reconstitution by consumers, or as ingredients in a variety of recombined applications, such as beverages, ice cream, confectionary and bakery products (Sharma *et al.*, 2012; Vignolles *et al.*, 2007).

The formulation of these fat-filled milk emulsions (FFMEs) prior to spray-drying typically involves blending of skim milk concentrate (SMC; *i.e.*, a concentrated protein and lactose solution) with oils (*i.e.*, often derived from plants, such as coconut or palm oils) to achieve the required ratio of protein to fat, and with additional carbohydrates added (Sharma *et al.*, 2012). SMC is produced by removal of the fat from milk through centrifugation and concentrating the remaining stream to a solids content of >35% (w/w) (O'Connell & Flynn, 2007). FFMEs are typically prepared by injecting fats into SMC, followed by emulsification using two-stage valve homogenisation. The fats that are used are typically derived from plants and are either solid or semi-solid at ambient temperature, in order to be comparable to milk fat. Thus, prior to injection, these fats need to be liquefied and dosed into the SMC at elevated temperatures, in the range 50-60^{o}C usually (Vignolles *et al.*, 2007). The ratio of protein with

respect to a fixed fat content is influenced by addition of carbohydrates (which reduces the protein content), often maltodextrins; these are polysaccharides of variable chain length produced by partial hydrolysis of starch, which are defined by their dextrose equivalent (DE) value (Drapala *et al.*, 2016; Mulcahy *et al.*, 2016; O'Mahony *et al.*, 2017). Use of higher concentrations of protein (*e.g.*, >5% w/w) in emulsion systems, in comparison to lower concentrations of protein, yields smaller emulsion droplets which are more resistant to emulsion instability, due to greater coverage of the droplet interface, reducing the propensity towards coalescence and increasing the electrostatic repulsive interactions between protein-stabilised emulsion droplets (O'Sullivan *et al.*, 2014; O'Sullivan, Park, & Beevers, 2016). Furthermore, dairy-derived carbohydrate sources, such as lactose or permeate from ultrafiltration of skim milk, are widely employed to vary the protein content with respect to fat in a similar fashion to maltodextrin addition. Plant-derived oils and maltodextrin ingredients are commonly used owing to their lower overall cost and reduced powder stickiness challenges during spray-drying, respectively (Gonzalez-Perez & Arellano, 2009; Vega & Roos, 2006).

After oil injection and emulsification, these formulations are spray-dried to yield FFMP (Sharma *et al.*, 2012). To the authors' knowledge, there are no studies available in the published literature detailing the formation of these high solids emulsion systems, the role of protein-to-fat ratio in their formation and stability, and the inline monitoring of this process from fat injection through to formation of the final emulsion. This study aims to investigate the emulsion formation process for high solids emulsions, using an inline high-shear mixer (IHSM) for emulsification, in a recirculation configuration (*i.e.*, semi-continuous), and to assess the suitability of using a pressure drop approach to monitor the process in real-time, from fat injection through to final emulsion formation.

High-shear mixers are widely used for emulsification applications and the dissolution of powders to form homogeneous solutions (Hall *et al.*, 2013; O'Sullivan *et al.*, 2017). The

configuration of these mixers is that of a rotor-stator, and they can be used in an inline configuration for either continuous processing (*i.e.*, single-pass mode) or semi-continuous processing (*i.e.*, multiple-pass mode), and are highly energy efficient (Hall *et al.*, 2011). The shear rate range for high-shear mixers is typically within the range 20,000 – 100,000 s^{-1}, depending on factors such as tip speed, rotor-stator geometry (*e.g.*, single or double screen) and physical properties (*e.g.*, viscosity, presence of particulates, etc.) of the material being processed (Pacek *et al.*, 2007). Pressure drop across a section of pipeline, for a flowing fluid, can be measured using a pair of pressure transducers, separated by a known distance. Pressure drop data provides useful information as to how a process is performing in real-time, as the data can be used to calculate a theoretical viscosity value from the Hagen-Poiseuille equation (Douglas *et al.*, 2005; Mihailova *et al.*, 2015). O'Sullivan *et al.* (2017) demonstrated the suitability of a pressure drop approach for monitoring the induction of dairy powders in real-time, observing different aspects of the process, such as initial contact of the powder with water, and the disintegration of powder particles as a function of processing time.

The overall objective of this research was to evaluate the suitability of the IHSM technology and discern differences in emulsification behaviour based on FFME formulation, in terms of emulsion fat droplet size distribution, emulsion viscosity and accelerated physical stability, as a function of processing time. Moreover, the emulsification process was monitored inline using a pressure drop approach, by applying the Hagen-Poiseuille equation. This approach allows for real-time monitoring of industrial emulsification processes, and provides information as to when dosing of oils is complete, as well as the progression of the emulsification process.

2. Materials and methods

2.1. Materials

Skim milk concentrate (SMC) and refined palm oil (RPO) were kindly provided by Dairygold Food Ingredients (Mitchelstown, Ireland). Maltodextrin with a dextrose equivalent (DE) value of 17 (MD17) was supplied by Corcoran Chemicals Ltd. (Dublin, Ireland). The composition of the SMC is presented in Table 1. The water used throughout this study was deionised water, unless stated otherwise.

2.2. Emulsion formulation and preparation

Emulsification was conducted at three protein concentrations, 7.7, 10.5 and 13% (w/w), with a fixed fat content of 12.1 ± 0.1% (w/w), whereby the % (w/w) level is based on total solids within a given system (*i.e.*, formulated emulsion or projected FFMP). Variations in emulsion formulation to meet these protein concentrations were achieved through addition of a fixed quantity of RPO and varying quantities of MD17 and water to SMC, as detailed in Table 1, with a target solids content of 52.3 ± 0.2% (w/w) in all cases. These protein contents were selected as the range in protein content for typical FFMP products is 14 to 24% (w/w) for the low to high protein contents, respectively (Sharma *et al.*, 2012). The predicted protein content of powders produced from the prepared emulsions would be 14.2, 19.2 and 23.7% (w/w) for the low-, medium- and high-protein systems, respectively, assuming that the final moisture content of the powder was 4% (w/w) in all cases (Table 1).

The configuration used for emulsification is shown in Fig. 1. The emulsification process was started by filling the closed-loop liquid system with the required amount of SMC to achieve the desired protein content for the investigated emulsion systems (Table 1), and initialising the progressive cavity pump (Torqueflow, Sydex, UK) at a volumetric flowrate of 675 L h^{-1}. Next, the inline high-shear mixer (IHSM), a YTRON-Z (1.50FC, YTRON Process Technology GmbH, Germany) operating at 100% capacity, yielding *ca.* 6,000 rpm, was initialised, and the custom-fabricated heat exchanger (Liam A. Barry Ltd., Cork, Ireland), in counter-current

123 configuration, was set to a temperature of 50°C. An overhead stirrer (RZR 2021, Heidolph
124 Instruments GmbH & Co. KG, Schwabach, Germany) at a speed of 1,000 rpm was used to
125 ensure rapid dispersion of MD17 powder and added water, and retained in place for the duration
126 of the emulsification process. The required mass of MD17 and water were carefully added to
127 the feed vessel over the top once the temperature of the recirculating SMC had reached 50°C
128 and the mixture was allowed to circulate through the system for a minimum of 30 min.
129 Subsequently, RPO was liquefied at a temperature of 50°C, the required mass was added to the
130 feed vessel over the top, and the mix was emulsified for up to 15 min (>50 passes through the
131 IHSM).

132 *2.3. Emulsion droplet size characterisation*

133 The changes in fat droplet size as a function of pass number (1, 3, 5, 10, 25 and 50
134 passes) through the IHSM were measured by static light-scattering using a Mastersizer 3000
135 (Hydro EV, Malvern Instruments, UK). Emulsion fat droplet size was reported as $d_{4,3}$ (*i.e.*,
136 volume-weighted mean droplet size), d_{10} (*i.e.*, cumulative 10% point of diameter), d_{50} (*i.e.*,
137 cumulative 50% point of diameter), d_{90} (*i.e.*, cumulative 90% point of diameter), droplet size
138 distribution data (DSD; volume vs. size class), and span (*i.e.*, width of the droplet size
139 distribution). *Eq.* 1 was used in order to determine the times required to achieve the desired
140 number of passes of the emulsion through the IHSM (O'Sullivan *et al.*, 2015):

141 $$t = \frac{V \times Pass\ number}{Q} \quad (1)$$

142 where t is the residence time (s), V is the volume within the system (m^3), and Q is the volumetric
143 flow rate ($m^3\ s^{-1}$).

2.4. Viscosity determination: comparison of calculated and experimental approaches

Viscosity was calculated from experimentally measured pressure drop (ΔP) readings, and compared to experimentally measured viscosity, in order to validate the calculated viscosity results, using a similar approach to that described by O'Sullivan *et al.* (2017). Pressure drop was recorded for the emulsification process, at all protein:fat ratios, and was recorded using a pair of pressure transducers (PR-33X, Keller, UK), positioned 1.08 m apart (Fig. 1). Pressure differential data was collected before dosage of molten RPO and for up to 15 min during the emulsification process. Calculated viscosity values were determined from *Eq.* 2, the Hagen-Poiseuille equation, using experimentally-measured pressure drop values, as follows (Douglas *et al.*, 2005; O'Sullivan *et al.*, 2017):

$$\eta_{calculated} = \frac{\pi \Delta P d^4}{128 L Q} \quad (2)$$

where $\eta_{calculated}$ is the calculated viscosity (Pa.s), ΔP is the pressure differential across a given straight section of pipeline (Pa), d is the internal diameter (19.05 mm), L is the length over which the pressure drop was recorded (1.08 m), and Q is the volumetric flow rate ($m^3\ s^{-1}$).

The experimental viscosity ($\eta_{experimental}$) was measured for all emulsion systems, after 1 and 50 passes, using a rotational viscometer (RST-CC Touch™, Brookfield AMETEK, Middleboro, MA, USA) equipped with a cup-and-bob geometry. Apparent viscosity was measured at 50°C (*i.e.*, the mean temperature at which emulsification was conducted; Section 2.2). A shear rate of 300 s^{-1} was used for viscosity determination, as this was determined to be similar to the shear rate in the pipeline between the pair of pressure transducers; the calculated shear rate within the 1.08 m section from which the pressure drop was recorded was 275 s^{-1}, determined using *Eq.* 3 (Douglas *et al.*, 2005):

$$\dot{\gamma} = \frac{8v}{d}, where\ v = \frac{Q}{A} \quad (3)$$

where $\dot{\gamma}$ is the shear rate (s^{-1}), d is the internal diameter (19.05 mm), v is the average velocity (m s^{-1}), Q is the volumetric flowrate (m^3s^{-1}), and A is the cross-sectional area (m^2).

2.5. Accelerated physical stability analysis of emulsions

Separation rates of FFMEs collected after 1 and 50 passes of aqueous and oil phases through the IHSM were measured using an analytical centrifuge (LUMiSizer, L.U.M. GmbH, Berlin, Germany). The principle of analysis by LUMiSizer has been detailed by Lerche and Sobisch (2011). Stability of emulsions to separation (i.e., creaming and sedimentation) driven by difference in the density between fat globules, undissolved powder and protein aggregates and the aqueous phase was determined at 23°C and 563 g over 500 min (i.e., 8 h 20 min) as detailed by Shimoni *et al.* (2013). Separation rates were calculated from integral transmission (IT) profiles using the initial linear ($R^2 \geq 0.95$) region of the slope of the plot of integral transmission *vs*. measurement time. Separation profiles (*i.e.*, the Space- and Time-resolved Extinction Profiles, STEP; Lerche and Sobisch, 2011) were collected at 10 min intervals during accelerated testing of emulsions to give information on changes in the light transmission through the measurement cell as a function of the specific position in the cell and, effectively, indicating progressive migration of emulsion components (*i.e.*, creaming and/or sedimentation).

2.6. Statistical analysis

Presented data are the average and standard deviation of at least three repeat measurements, and from a single production run of SMC, RPO and MD17. Student's t-test with a 95% confidence interval analysis was performed using Microsoft Excel and was used to assess the significance of the results obtained, whereby t-test differences with $P < 0.05$ were considered statistically significant.

3. Results and discussion

3.1. Effect of pass number through the inline high-shear mixer (IHSM) on fat droplet size distribution

The effect of pass number through the IHSM (*i.e.*, residence time within the shear field) on fat droplet size distribution was assessed for low-, medium- and high-protein FFMEs (Fig. 2 and Table 2). After a single pass through the IHSM, large fat droplets were found; the medium-protein FFME yielded the smallest initial droplets ($d_{4,3}$ of 6.67 ± 0.31 μm), while the high-protein FFME yielded the largest initial droplet size ($d_{4,3}$ of 9.62 ± 0.79 μm). This may be explained by the fact that moderate concentrations of protein allow for more efficient adsorption and stabilisation of oil-water interfacial layers, yielding smaller emulsion droplets (Beverung *et al.*, 1999; O'Sullivan, Beevers *et al.*, 2015). As these samples were further processed (*i.e.*, with increasing pass number), the size of the fat droplets (in particular d_{50} and d_{90}; Table 2) decreased significantly ($P < 0.05$), for all protein contents investigated.

Furthermore, the extent of droplet size reduction was greatest for the low-protein emulsions, in terms of d_{50} and d_{90}, throughout the entire process. This behaviour was attributed to the higher viscosity of the continuous phase of those systems in comparison to that of the medium- and high-protein samples, allowing for greater ease of disruption of fat droplets (Lee *et al.*, 2013; Walstra, 1993). A higher viscosity difference between the continuous and dispersed phases (*i.e.*, viscosity ratio), results in enhanced droplet breakup within the turbulent flow regimes observed for the IHSM (Walstra & Smulders, 2000). Furthermore, the primary mode of droplet breakup within the IHSM results from the high degree of turbulence, which causes chaotic velocity fields, resulting in turbulent eddies, characterised by the Kolmogorov length scale (Walstra, 1993).

In addition, in all cases, and for any given time point in the process, a bimodal size distribution was observed (Fig. 2), in which the micron-sized peak (*ca.* 5 μm after 50 passes) was ascribed to emulsion fat droplets, whereas the submicron peak (*ca.* 250 nm) was associated with casein micelles, the dominant protein fraction of SMC (O'Sullivan *et al.*, 2017). After 25 passes through the IHSM, the low-protein (7.7% w/w) emulsion had droplets ≤ 10 μm (Fig. 2a), while droplets > 10 μm were still present in the medium- (Fig. 2b) and high-protein (Fig. 2c) emulsions even after 50 passes through the IHSM. It is also worth noting that the low-protein emulsion had the narrowest droplet size distribution (DSD; Fig. 2a), irrespective of the number of passes through the IHSM, as also evident from the lowest span values for this emulsion (Table 2), compared to medium- and high-protein emulsions. This is thought to be associated with the higher viscosity of the continuous phase of the low-protein content FFME, in comparison to the other protein contents. The reduction of emulsion droplet size as a function of pass number was similarly demonstrated for a range of other emulsification processes, including IHSMs (Hall *et al.*, 2011), continuous ultrasonic processors (O'Sullivan *et al.*, 2015), high-pressure valve homogenisers (Lee & Norton, 2013) and microfluidizers (Lee & Norton, 2013).

3.2. Inline assessment of emulsification using the pressure drop approach

The calculated viscosity ($\eta_{calculated}$) as a function of pass number (up to 50 passes) was investigated and is shown in Fig. 3 for FFMEs prepared at low-, medium- and high-protein concentrations. Upon addition of molten RPO to the emulsification system (Fig. 1), there was a significant increase ($P < 0.05$) in $\eta_{calculated}$ for all of the investigated formulations, where this behaviour was ascribed to the increased solids content within the system, resulting in an increased pressure differential and thus $\eta_{calculated}$ (Douglas *et al.*, 2005; O'Sullivan *et al.*, 2017). Following the addition of fat, $\eta_{calculated}$ decreased marginally as a function of pass number, in particular for the medium-protein FFME. This behaviour was attributed to the reduction of fat

droplet size, which is known to result in a reduced viscosity for emulsion systems (McClements, 2005). Thus, the emulsification process exhibited two distinct stages in all instances, an initial significant ($P < 0.05$) increase, followed by a gradual reduction to a final viscosity value. These distinct stages correspond to: (i) an increase in the solids content of the system due to the introduction of molten fat to the skim milk concentrate (SMC), and (ii) size reduction of fat droplets with successive passes through the IHSM.

Furthermore, when comparing $\eta_{calculated}$ values after 50 passes for each FFME formulation, the low-protein emulsion exhibited, unexpectedly, the highest viscosity value (36.5 ± 1.3 mPa.s), followed by the high-protein emulsion, with a marginally lower viscosity value (34.7 ± 2.2 mPa.s), and the medium-protein sample, which had a significantly lower ($P < 0.05$) viscosity (29.2 ± 0.7 mPa.s), in comparison to both the low- and high-protein systems. Even though all of the systems had the same solids content (52.5% w/w; Table 1), the factor which dictated the resultant value of $\eta_{calculated}$ was thought to be the concentration of MD17, rather than the protein content. MD17 has an average molecular weight of 24.9 kDa (Chen & O'Mahony, 2016; Rong *et al.*, 2009), and maltodextrin has a highly branched structure consisting of D-glucose monomer units (Avaltroni *et al.*, 2004; Chronakis, 1998; Wang & Wang, 2000); in addition, individual molecules of MD17 interact with one another, contributing to increases in viscosity with increasing concentration (Avaltroni *et al.*, 2004; Morris *et al.*, 1981). The intrinsic viscosity ([η]; *i.e.*, hydrodynamic volume) of MD17 is significantly greater than that of the proteins in SMC, *ca.* 80:20 mixture of casein micelles and whey protein, the same as observed in milk protein isolates (MPI) (O'Connell & Flynn, 2007; Vos *et al.*, 2016), whereby the $[\eta]_{MD17}$ was 3.5 dL g^{-1}, in comparison to $[\eta]_{MPI}$ which had a value of 0.59 dL g^{-1} (Avaltroni *et al.*, 2004; O'Sullivan *et al.*, 2014). The significantly ($P < 0.05$) higher value of $[\eta]_{MD17}$ highlights that MD17 would have a more pronounced effect on the resultant viscosity of FFMEs than the protein component. Thus, the higher concentration

of MD17 in the low-protein content emulsion yielded the highest viscosity and, as the concentration of MD17 decreased, and that of protein increased, there was a significant ($P < 0.05$) decrease in viscosity. Moreover, as the concentration of MD17 further decreased, and the concentration of protein increased, the protein component becomes the dominant influencer of viscosity, in comparison to MD17; nevertheless, the resultant viscosity remained lower than that of the low-protein emulsion system (Fig. 3).

The validity of the $\eta_{calculated}$ results was assessed through direct comparison of experimentally obtained viscosity values measured at a shear rate of 300 s^{-1}, a value close to that at which the pressure drop was measured (275 s^{-1}), and at the average temperature recorded during emulsification (50°C). The values of $\eta_{calculated}$ and experimental viscosity ($\eta_{experimental}$) for all of the investigated FFME systems, after 1 and 50 passes, are shown in Table 3. The trend of $\eta_{experimental}$ for all of the FFMEs is comparable to that of $\eta_{calculated}$, whereby the low-protein system possessed the highest apparent viscosity and the medium-protein emulsion exhibited the lowest viscosity, for the same reasons as previously discussed, associated with differences in MD17 concentration. Furthermore, the viscosity values for 1 pass were significantly ($P < 0.05$) lower than those at 50 passes, which is in agreement with $\eta_{calculated}$ values as a function of time (Fig. 3). This behaviour is ascribed to either the fact that the RPO has not had sufficient time to form a uniform emulsion after a single pass (< 14 s), or potential increased levels of hydration of MD17 resulting from the shearing process.

A comparison of the $\eta_{calculated}$ and $\eta_{experimental}$ values for all FFME systems highlight that there is a discrepancy in the values, by a factor of *ca.* 1.25, whereby the calculated value represents an overestimation in all instances. This observed difference between calculated and experimental values was ascribed to the nature of the Hagen-Poiseuille equation, which assumes that the fluid exhibits Newtonian behaviour, whereas it has been established that highly concentrated (52.5% solids, w/w) emulsion systems demonstrate pseudoplastic

288 rheological behaviour (O'Sullivan *et al.*, 2016; Pal, 1996, 2011). A similar trend was observed
289 by O'Sullivan *et al.* (2017) for the induction and dissolution of dairy powders, whereby the
290 difference between calculated and experimental viscosity values was a factor of 2, which was
291 also ascribed to the non-Newtonian behaviour of dairy solutions.

292 *3.3. Accelerated physical stability of emulsions*

293 Differences in the extent of phase separation in FFME systems after 1 and 50 passes
294 through the IHSM tested under accelerated conditions (563 g for 500 min) were clear from the
295 space- and time-resolved extinction profiles (STEP; Fig. 4). After the 1st pass through the
296 IHSM, only limited differences in phase separation were observed between all emulsions. More
297 pronounced differences in separation were observed for emulsions after 50 passes through the
298 IHSM, where the low-protein (7.7%, w/w) emulsion displayed lowest separation, followed by
299 emulsions with high- (13%, w/w) and medium-protein (10.5%, w/w) levels (Fig. 4). Separation
300 of formulations was identified as being mostly due to the migration of fat globules towards the
301 top of the measuring cell (*i.e.*, creaming) as evidenced by a progressive appearance of a cream
302 layer and only a limited sediment build-up in all samples (Fig. 4). Creaming and sedimentation
303 were reduced on progressive recirculation through the IHSM system, due to decreases in the
304 size of fat globules and enhanced hydration of the MD17 powder (O'Sullivan *et al*., 2016).

305 Similar emulsion separation trends were observed for the integral transmission (IT)
306 profiles (Fig. 5); the IT represents separation in the samples due to both creaming (upward
307 movement of the less dense phase, i.e., fat droplets, and downward movement of the more
308 dense solutes, i.e., maltodextrin and protein). The evolution of separation increased in the order
309 of low-protein 50th pass < high-protein 50th pass < medium-protein 50th pass < high-protein 1st
310 pass < medium-protein 1st pass < low-protein 1st pass. Despite lack of significant differences
311 in the initial (*i.e.*, first 45 min) slopes of increasing transmission for emulsions after 50 passes

312 through the IHSM (Table 2), the overall (*i.e.*, during 500 min) separation of the low-protein
313 emulsion was lower than that of both medium- and high-protein emulsions after 50 passes (Fig.
314 5). This can be explained by the greater population of smaller particles (*i.e.*, fat globules; Fig.
315 2, Table 2) in the low-protein content emulsion after 50 passes, compared to the other
316 emulsions after 50 passes, causing divergence of the IT profiles after initial movement of the
317 larger particles (*i.e.*, bigger particles move first and smaller particles move more slowly).

318 The results for the accelerated emulsion separation closely correlate with those obtained
319 for DSD and apparent viscosity of the FFME systems, whereas, in accordance with Stoke's
320 Law, emulsions with largest droplet size and lowest viscosity also displayed the most rapid
321 separation. The low-protein emulsion after 50 passes had the highest apparent viscosity,
322 compared to the other emulsions (Table 3), further enhancing stability of the emulsion to
323 density-driven separation.

324 **4. Conclusions**

325 Inline high-shear mixing (IHSM) was shown to be an effective approach for the
326 preparation of fat-filled milk emulsions (FFMEs). The most effective emulsification, as a
327 function of pass number, was achieved for the low-protein FFME, as observed by the formation
328 of smaller emulsion droplets, which was ascribed to the enhanced droplet breakup due to the
329 increased viscosity differential between the dispersed and continuous phases. Inline
330 measurement of pressure drop is thus an effective approach for monitoring real-time
331 emulsification kinetics of refined palm oil (RPO) in skim milk concentrate (SMC). Pressure
332 drop data was used to determine real-time viscosity, by means of the Hagen-Poiseuille
333 equation; after emulsification, the low-protein FFME exhibited the highest viscosity in
334 comparison to the other systems, which was ascribed to lower and narrower DSD and to the
335 higher content of MD17 and its associated higher intrinsic viscosity in comparison to the

336 protein component of the formulations. The lowest viscosity was exhibited by the medium-
337 protein FFME, associated with the reduction in MD17 concentration. The emulsification
338 process exhibited two distinct phases as observed by pressure drop results: (i) initial injection
339 of fat, and (ii) fat droplet reduction in the shear mixing field.

340

341 **Acknowledgements**

342 The authors would like to acknowledge the Dairy Processing Technology Centre
343 (DPTC), an Enterprise Ireland initiative, for financial support and permission to publish this
344 work. This work was supported by the Irish State through funding from the Technology Centres
345 programme (Grant Number TC/2014/0016). The authors would like to thank Dr Olga
346 Mihailova of Unilever Research (Port Sunlight, UK) for assistance with respect to data
347 processing. The authors would also like to thank Mike Barry and Kevin McEvoy of Liam A.
348 Barry Ltd. (Cork, Ireland) for the custom fabrication of many of the stainless steel components
349 of the experimental setup.

350

351 **References**

352 Avaltroni, F., Bouquerand, P. E., & Normand, V. (2004). Maltodextrin molecular weight
353 distribution influence on the glass transition temperature and viscosity in aqueous
354 solutions. *Carbohydrate Polymers*, *58*(3), 323–334.

355 Beverung, C. J., Radke, C. J., & Blanch, H. W. (1999). Protein adsorption at the oil/water
356 interface: characterization of adsorption kinetics by dynamic interfacial tension
357 measurements. *Biophysical Chemistry*, *81*(1), 59–80.

358 Chen, B., & O'Mahony, J. A. (2016). Impact of glucose polymer chain length on heat and

physical stability of milk protein-carbohydrate nutritional beverages. *Food Chemistry*, *211*, 474–482.

Chronakis, I. S. (1998). On the molecular characteristics, compositional properties, and structural-functional mechanisms of maltodextrins: a review. *Critical Reviews in Food Science and Nutrition*, *38*(7), 599–637.

Douglas, J., Gasoriek, J., Swaffield, J., & Jack, L. (2005). *Fluid Mechanics* (5th ed.). Essex, UK: Prentice Hall.

Drapala, K. P., Auty, M. A. E., Mulvihill, D. M., & O'Mahony, J. A. (2016). Performance of whey protein hydrolysate-maltodextrin conjugates as emulsifiers in model infant formula emulsions. *International Dairy Journal*, *62*, 76–83. https://doi.org/10.1016/j.idairyj.2016.03.006

Fox, P. F. (2008). Chapter 1 - Milk: an overview. In A. Thompson, M. Boland, H. Singh, A. Thompson, & M. Boland (Eds.) (pp. 1–54). San Diego: Academic Press.

Gonzalez-Perez, S., & Arellano, J. B. (2009). Vegetable protein isolates. In G. O. Philips & P. A. Williams (Eds.), *Handbook of Hydrocolloids* (2nd ed., pp. 383–419). Cambridge, UK: Woodhead Publishing Limited.

Hall, S., Cooke, M., El-Hamouz, A., & Kowalski, A. J. (2011). Droplet break-up by in-line Silverson rotor–stator mixer. *Chemical Engineering Science*, *66*(10), 2068–2079.

Hall, S., Pacek, A. W., Kowalski, A. J., Cooke, M., & Rothman, D. (2013). The effect of scale and interfacial tension on liquid–liquid dispersion in in-line Silverson rotor–stator mixers. *Chemical Engineering Research and Design*, *91*(11), 2156–2168. https://doi.org/10.1016/j.cherd.2013.04.021

Lee, L. L., Niknafs, N., Hancocks, R. D., & Norton, I. T. (2013). Emulsification: Mechanistic

382 understanding. *Trends in Food Science & Technology*, *31*(1), 72–78.
383 https://doi.org/10.1016/j.tifs.2012.08.006

384 Lee, L., & Norton, I. T. (2013). Comparing droplet breakup for a high-pressure valve
385 homogeniser and a Microfluidizer for the potential production of food-grade
386 nanoemulsions. *Journal of Food Engineering*, *114*(2), 158–163.
387 https://doi.org/http://dx.doi.org/10.1016/j.jfoodeng.2012.08.009

388 Lerche, D., & Sobisch, T. (2011). Direct and Accelerated Characterization of Formulation
389 Stability. *Journal of Dispersion Science and Technology*, *32*(12), 1799–1811.
390 https://doi.org/10.1080/01932691.2011.616365

391 McClements, D. J. (2005). *Food Emulsions: Principles, Practices, and Techniques* (2nd ed.).
392 CRC Press.

393 Mihailova, O., Lim, V., McCarthy, M. J., McCarthy, K. L., & Bakalis, S. (2015). Laminar
394 mixing in a SMX static mixer evaluated by positron emission particle tracking (PEPT)
395 and magnetic resonance imaging (MRI). *Chemical Engineering Science*, *137*, 1014–
396 1023.

397 Morris, E. R., Cutler, A. N., Ross-Murphy, S. B., Rees, D. A., & Price, J. (1981).
398 Concentration and shear rate dependence of viscosity in random coil polysaccharide
399 solutions. *Carbohydrate Polymers*, *1*, 5–21.

400 Mulcahy, E. M., Mulvihill, D. M., & O'Mahony, J. A. (2016). Physicochemical properties of
401 whey protein conjugated with starch hydrolysis products of different dextrose equivalent
402 values. *International Dairy Journal*, *53*, 20–28.
403 https://doi.org/10.1016/j.idairyj.2015.09.009

404 O'Connell, J. E., & Flynn, C. (2007). The manufacture and application of casein-derived

ingredients. In Y. H. Hui (Ed.), *Handbook of Food Products Manufacturing* (1st ed., pp. 557–593). New Jersey: John Wiley & Sons.

O'Mahony, J. A., Drapala, K. P., Mulcahy, E. M., & Mulvihill, D. M. (2017). Controlled glycation of milk proteins and peptides: Functional properties. *International Dairy Journal*, *67*, 16–34.

O'Sullivan, J., Arellano, M., Pichot, R., & Norton, I. (2014). The effect of ultrasound treatment on the structural, physical and emulsifying properties of dairy proteins. *Food Hydrocolloids*, *42*(3), 386–396.

O'Sullivan, J., Beevers, J., Park, M., Greenwood, R., & Norton, I. (2015). Comparative assessment of the effect of ultrasound treatment on protein functionality pre- and post-emulsification. *Colloids and Surfaces A: Physicochemical and Engineering Aspects*, *484*, 89–98. https://doi.org/10.1016/j.colsurfa.2015.07.065

O'Sullivan, J. J., & O'Mahony, J. A. (2016). Food Ingredients. In *Reference Module in Food Science* (pp. 1–3). Amsterdam, Netherlands: Elsevier.

O'Sullivan, J. J., Schmidmeier, C., Drapala, K. P., O'Mahony, J. A., & Kelly, A. L. (2017). Monitoring of pilot-scale induction processes for dairy powders using inline and offline approaches. *Journal of Food Engineering*, *197*, 9–16.

O'Sullivan, J., Murray, B., Flynn, C., & Norton, I. (2015). Comparison of batch and continuous ultrasonic emulsification processes. *Journal of Food Engineering*, *167(B)*, 141–121.

O'Sullivan, J., Murray, B., Flynn, C., & Norton, I. T. (2016). The effect of ultrasound treatment on the structural, physical and emulsifying properties of animal and vegetable proteins. *Food Hydrocolloids*, *53*, 141–154.

O'Sullivan, J., Park, M., & Beevers, J. (2016). The effect of ultrasound upon the physicochemical and emulsifying properties of wheat and soy protein isolates. *Journal of Cereal Science*.

Pacek, A., Baker, M., & Utomo, A. (2007). Characterisation of flow pattern in a rotor stator high shear mixer. In *Proceedings of European Congress of Chemical Engineering (ECCE-6)*.

Pal, R. (1996). Effect of droplet size on the rheology of emulsions. *AIChE Journal*, *42*(11), 3181–3190. https://doi.org/10.1002/aic.690421119

Pal, R. (2011). Rheology of simple and multiple emulsions. *Current Opinion in Colloid & Interface Science*, *16*(1), 41–60. https://doi.org/10.1016/j.cocis.2010.10.001

Rong, Y., Sillick, M., & Gregson, C. M. (2009). Determination of dextrose equivalent value and number average molecular weight of maltodextrin by osmometry. *Journal of Food Science*, *74*(1), C33–C40. https://doi.org/10.1111/j.1750-3841.2008.00993.x

Sharma, A., Jana, A. H., & Chavan, R. S. (2012). Functionality of Milk Powders and Milk-Based Powders for End Use Applications-A Review. *Comprehensive Reviews in Food Science and Food Safety*, *11*(5), 518–528. https://doi.org/10.1111/j.1541-4337.2012.00199.x

Shimoni, G., Shani Levi, C., Levi Tal, S., & Lesmes, U. (2013). Emulsions stabilization by lactoferrin nano-particles under in vitro digestion conditions. *Food Hydrocolloids*, *33*(2), 264–272. https://doi.org/10.1016/j.foodhyd.2013.03.017

Vega, C., & Roos, Y. H. (2006). Invited review: spray-dried dairy and dairy-like emulsions--compositional considerations. *Journal of Dairy Science*, *89*(2), 383–401. https://doi.org/10.3168/jds.S0022-0302(06)72103-8

Vignolles, M.-L., Jeantet, R., Lopez, C., & Schuck, P. (2007). Free fat, surface fat and dairy powders: interactions between process and product. A review. *Le Lait*, *87*(3), 187–236. https://doi.org/10.1051/lait:2007010

Vos, B., Crowley, S. V., O'Sullivan, J., Evans-Hurson, R., McSweeney, S., Krüse, J., … O'Mahony, J. A. (2016). New insights into the mechanism of rehydration of milk protein concentrate powders determined by Broadband Acoustic Resonance Dissolution Spectroscopy (BARDS). *Food Hydrocolloids*, *61*, 933–945.

Walstra, P. (1993). Principles of emulsion formation. *Chemical Engineering Science*, *48*(2), 333–349. https://doi.org/http://dx.doi.org/10.1016/0009-2509(93)80021-H

Walstra, P., & Smulders, P. (2000). Emulsion Formation. In B. . Binks (Ed.), *Modern Aspects of Emulsion Science* (1st ed., pp. 56–99). Cambridge, UK: The Royal Society of Chemistry.

Wang, Y.-J., & Wang, L. (2000). Structures and Properties of Commercial Maltodextrins from Corn, Potato, and Rice Starches. *Starch - Stärke*, *52*(8–9), 296–304. https://doi.org/10.1002/1521-379X(20009)52:8/9<296::AID-STAR296>3.0.CO;2-A

1 Fig. 1.

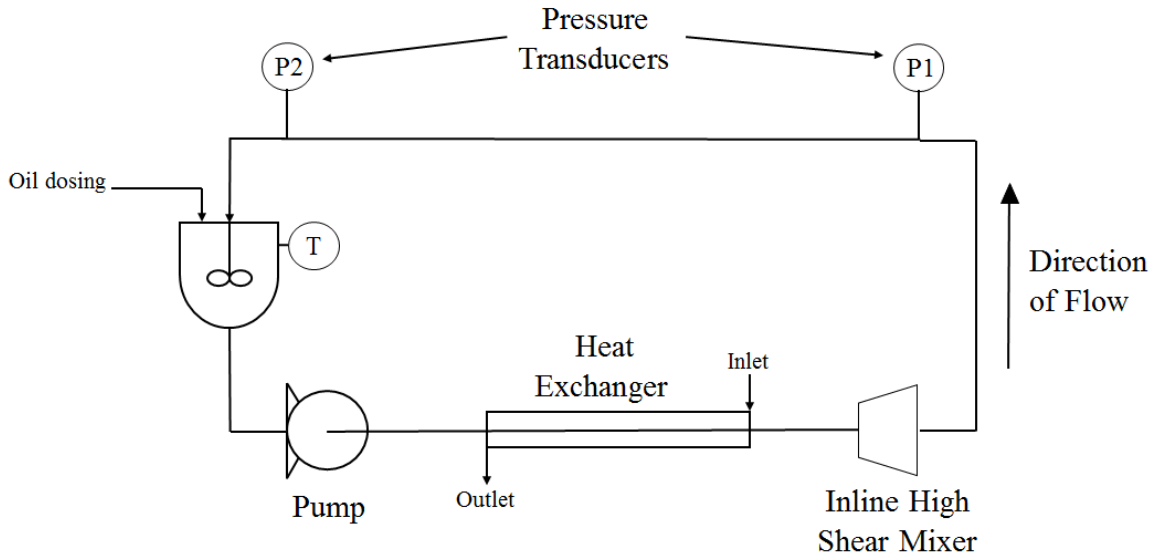

2

1 Fig. 2.

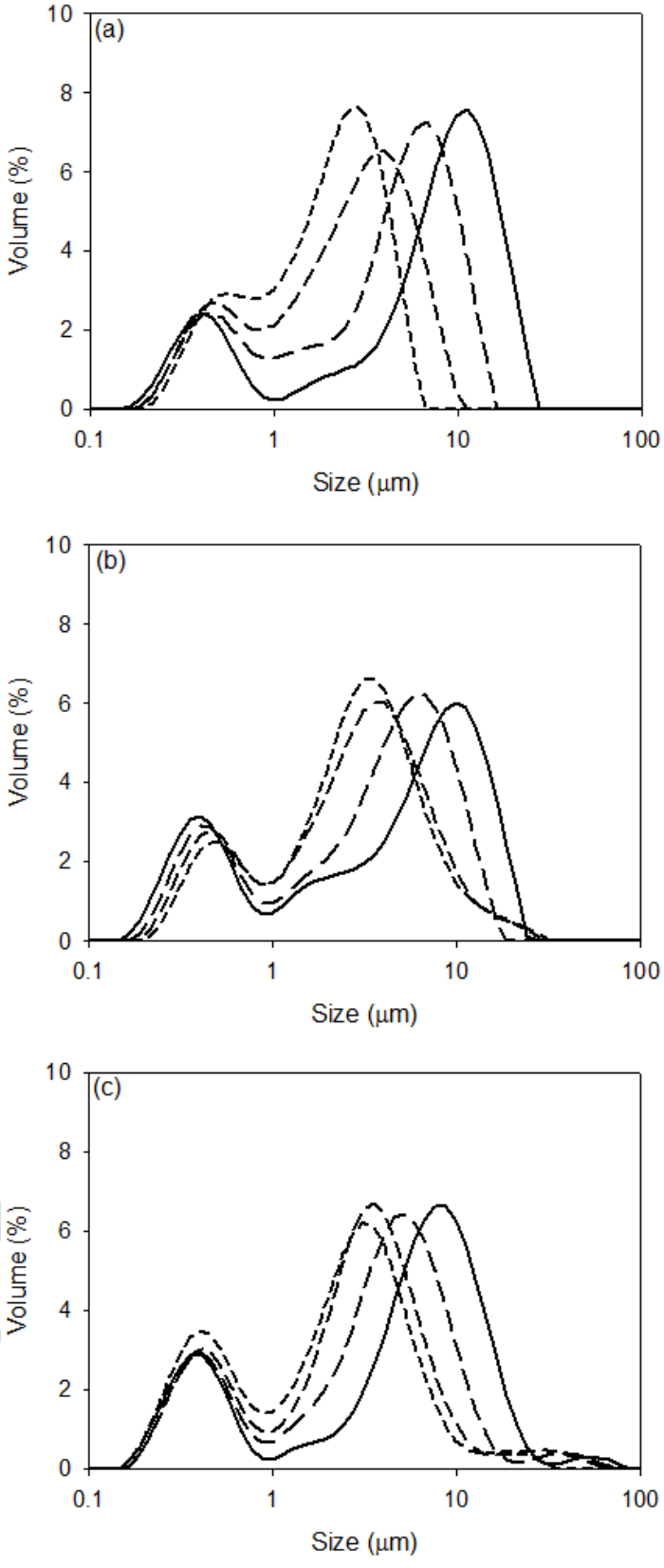
(a)
Volume (%)
Size (μm)
(b)
Volume (%)
Size (μm)
(c)
Volume (%)
Size (μm)
0
2
4
6
8
10
0.1
1
10
100

2

1 Fig. 3.

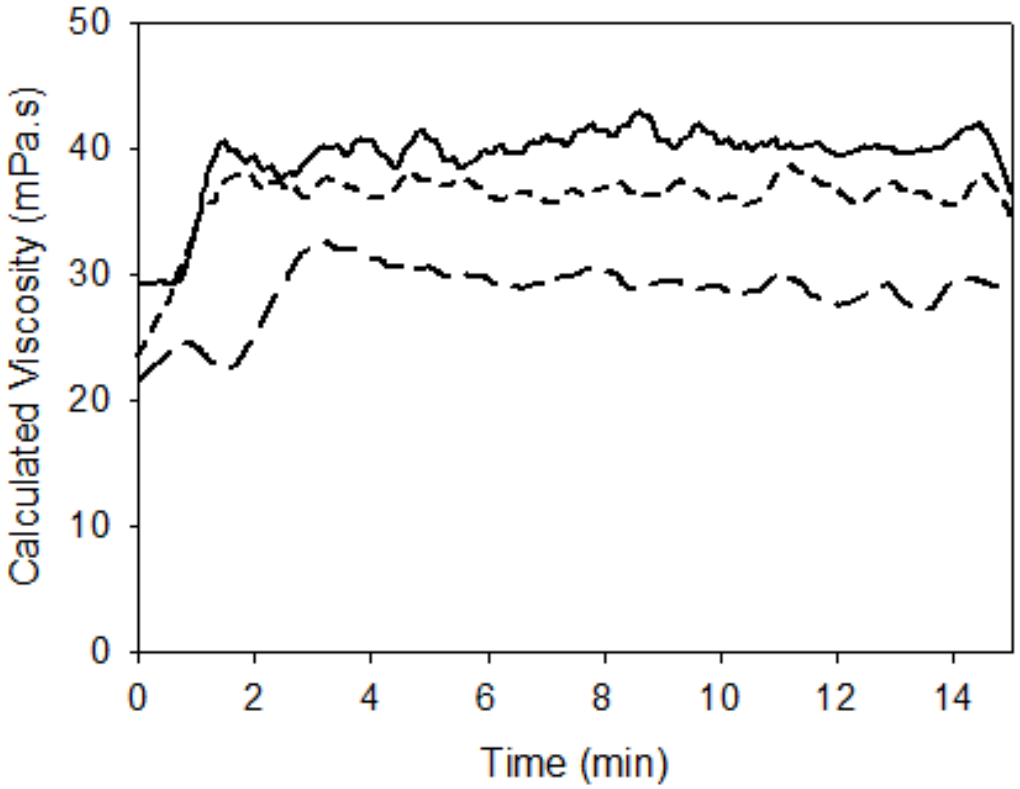

2

1 Fig. 4.

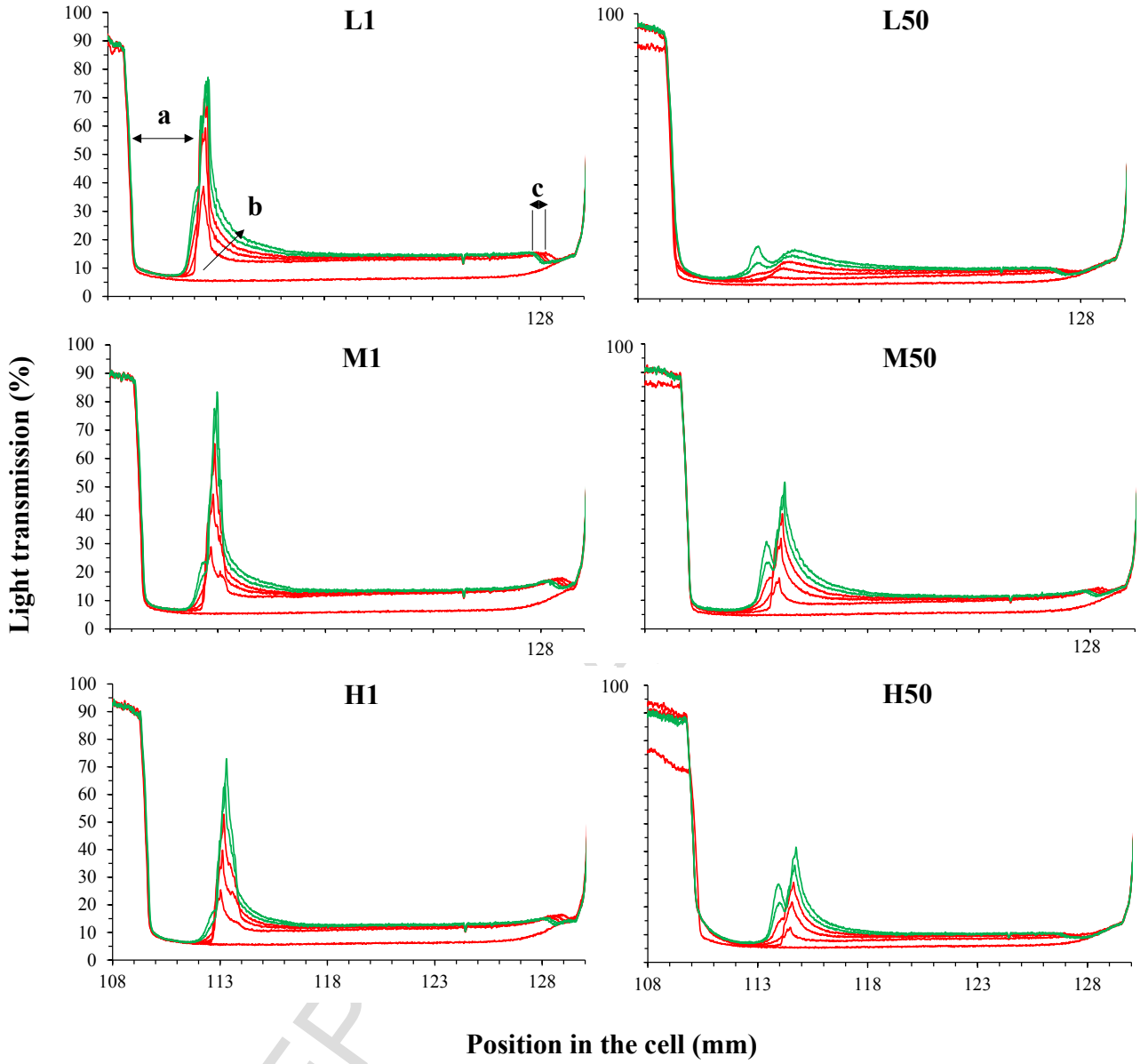

2
3

1 Fig. 5.

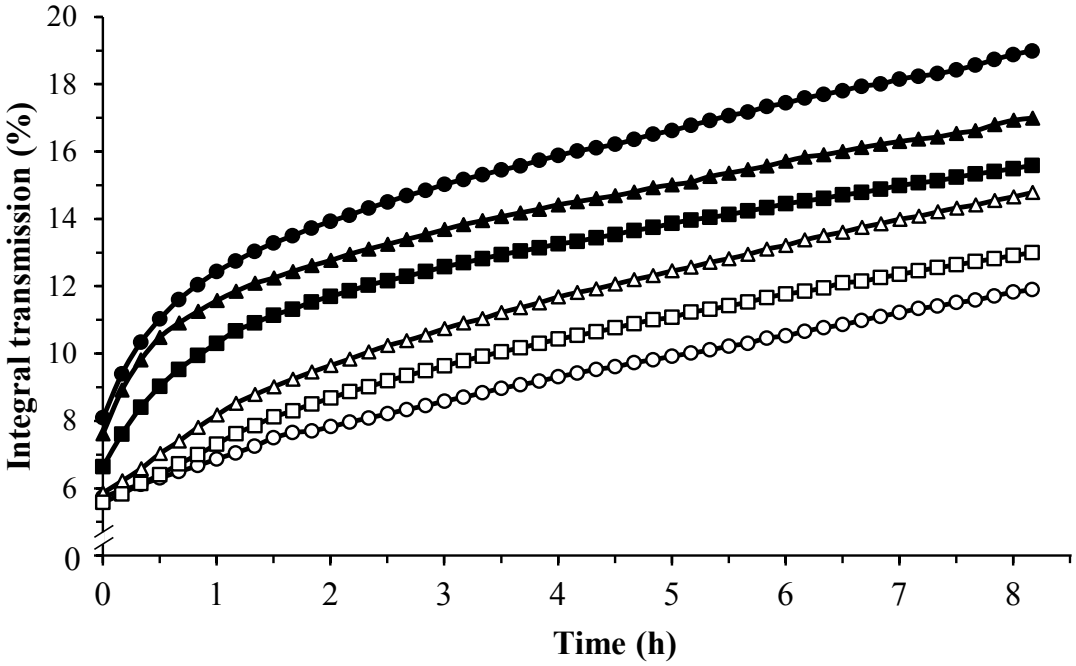

2
3

Figure captions

Fig. 1. Schematic representation of the experimental configuration employed, showing the inline high-shear mixer, heat exchanger, pressure transducers, batch vessel and pump.

Fig. 2. Changes in oil droplet size distribution as a function of pass number through the inline high-shear mixer, showing data for 1 (solid line), 5 (long-dashed line), 25 (medium-dashed line), and 50 (short-dashed line) passes after dosing of refined palm oil for: (a) low-protein fat-filled milk emulsions (FFME), (b) medium-protein FFME, and (c) high-protein FFME. The concentration of refined palm oil in all cases was 12% (w/w).

Fig. 3. Calculated viscosity upon addition of molten refined palm oil to the system as a function of time for low-protein fat-filled milk emulsions (FFME) (solid line), medium-protein FFME (long-dashed line), and high-protein FFME (short-dashed line). The concentration of refined palm oil in all cases was 12% (w/w).

Fig. 4. Emulsion separation profiles for low- (L), medium- (M) and high-protein (H) fat-filled milk emulsions (FFMEs) after 1 and 50 passes through the inline high-shear mixer. The profiles demonstrate changes in the transmission of light trough the sample cell due to migration of its component under centrifugal acceleration. The sample is contained between the position 110 mm (top of the cell) and position 129 mm (bottom of the cell). The evolution of the transmission profiles over the duration of the analysis is represented by the arrow (b), where the phase boundary progressively moves towards the bottom of the cell while the thickness of the cream layer increases (a) and the sediment layer builds-up (c). Colours indicate the sequence of the profiles (RED profiles were collected early, first profile at time 0 min; GREEN profiles were collected late in separation, last profile collected at time 500 min – please refer to on-line version for full colour Figure).

Fig. 5. Separation profiles expressed as integral transmission as a function of time for fat-filled milk emulsions (FFMEs) with low- (circle), medium- (triangle) and high-protein (square) after 1 (solid fill) and 50 (no fill) passes through the inline high-shear mixer as measured using the LUMiSizer analytical centrifuge.

Table 1.

Composition of skim milk concentrate (SMC), low-, medium- and high-protein fat-filled milk emulsions (FFME), and calculated composition of resultant low-, medium- and high-protein content fat-filled milk powders (FFMP).

		Fat-Filled Milk Emulsions			Fat-Filled Milk Powders		
	SMC	Low	Medium	High	Low	Medium	High
Protein (%)	16.2	7.7	10.5	13	14.2	19.2	23.7
Fat (%)	0.4	12.2	12.2	12	22.4	22.3	22.1
Lactose (%)	23.1	11.4	14.9	18.6	21	27.2	34
Maltodextrin (%)	0	20.3	14.2	8	37.4	26	14.6
Lactose + Maltodextrin (%)	23.1	31.7	29.1	26.6	58.4	53.2	48.6
Ash (%)	1.1	0.5	0.7	0.9	1	1.3	1.6
Water (%)	59.2	47.9	47.5	47.5	4	4	4

Table 2.

Effect of pass number (1, 5, 25 and 50) through the inline high-shear mixer on $d_{3,2}$ (*i.e.*, Sauter diameter), $d_{4,3}$ (*i.e.*, volume-weighted mean diameter), d_{10}, d_{50}, d_{90}, *span*, and separation rates, calculated from the initial linear response ($R^2 \geq 0.95$) of the slope of plots of integral transmission *vs.* measurement time, for low-, medium- and high-protein fat-filled milk emulsions (FFMEs).

Protein Content (% w/w)	Pass (-)	$d_{4,3}$ (μm)	d_{10} (μm)	d_{50} (μm)	d_{90} (μm)	*Span* (-)	*Rate of initial transmission increase* (%/h)
7.7	1	9.62 ± 0.79	0.45 ± 0.01	9.65 ± 0.05	17.4 ± 0.13	1.91 ± 0.02	7.69 ± 0.43
	5	5.47 ± 0.32	0.51 ± 0.01	4.91 ± 0.03	10.5 ± 0.04	2.04 ± 0.01	-
	25	3.08 ± 0.09	0.49 ± 0.02	2.65 ± 0.04	6.35 ± 0.05	2.17 ± 0.03	-
	50	2.31 ± 0.03	0.49 ± 0.03	2.11 ± 0.02	4.41 ± 0.03	1.82 ± 0.02	5.60 ± 0.05
10.5	1	6.67 ± 0.31	0.43 ± 0.04	5.76 ± 0.07	16.8 ± 0.09	2.89 ± 0.05	6.85 ± 0.35
	5	4.89 ± 0.08	0.51 ± 0.05	3.73 ± 0.04	12.3 ± 0.02	3.16 ± 0.02	-
	25	4.05 ± 0.02	0.52 ± 0.03	2.83 ± 0.02	8.21 ± 0.05	2.73 ± 0.01	-
	50	3.99 ± 0.06	0.65 ± 0.03	2.82 ± 0.01	6.85 ± 0.06	2.26 ± 0.02	5.47 ± 0.03
13	1	9.41 ± 0.87	0.37 ± 0.01	6.58 ± 0.09	15.4 ± 0.13	2.34 ± 0.06	6.16 ± 0.07
	5	6.22 ± 0.51	0.39 ± 0.01	4.15 ± 0.04	10.8 ± 0.05	2.42 ± 0.08	-
	25	4.52 ± 0.31	0.41 ± 0.01	3.04 ± 0.02	8.11 ± 0.07	2.57 ± 0.05	-
	50	3.74 ± 0.19	0.36 ± 0.01	2.52 ± 0.04	7.09 ± 0.06	2.74 ± 0.11	5.35 ± 0.12

Table 3.

Comparison of calculated viscosity (1 and 50 passes after dosing of molten refined palm oil) and experimentally measured viscosity (at a shear rate of 300 s^{-1}) for fat-filled milk emulsions with low-, medium- and high-protein contents. The concentration of refined palm oil in all cases was 12% (w/w).

Number of Passes (-)	Protein Content (% w/w)	$\eta_{calculated}$ (mPa.s)	$\eta_{experimental}$ (mPa.s)
1	7.7	29.1 ± 1.1	22.6 ± 0.2
	10.5	21.8 ± 0.8	13.5 ± 0.5
	13	23.9 ± 1.7	26.5 ± 2.9
50	7.7	36.5 ± 1.3	33.4 ± 0.5
	10.5	29.2 ± 0.7	15.9 ± 1.5
	13	34.7 ± 2.2	27.6 ± 3.2